Inherited retinal degenerations: clinical characterization on the road to therapy

Talib, M.

4.
RPGR-associated retinal dystrophies

4.1

Clinical and genetic characteristics of male patients with *RPGR*-associated retinal dystrophies: a long-term follow-up study

Mays Talib, MD[1], Mary J. van Schooneveld, MD, PhD[2], Alberta A. Thiadens, MD, PhD[3], Marta Fiocco, PhD[4,5], Jan Wijnholds, PhD[1], Ralph J. Florijn, PhD[6], Nicoline E. Schalij-Delfos, MD, PhD[1], Maria M. van Genderen, MD, PhD[7], H. Putter, PhD[4], Frans P.M. Cremers, PhD[8], Gislin Dagnelie, PhD[9], Jacoline B. ten Brink, BAS[6], Caroline C.W. Klaver, MD, PhD[3,10,11], L. Ingeborgh van den Born, MD, PhD[12], Carel B. Hoyng, MD, PhD[11], Arthur A. Bergen, PhD[6,13], Camiel J.F. Boon, MD, PhD[1,2]

Retina 2019;39(6):1186-1199

1 Department of Ophthalmology, Leiden University Medical Center, Leiden, The Netherlands.
2 Department of Ophthalmology, Academic Medical Center, Amsterdam, The Netherlands
3 Department of Ophthalmology, Erasmus Medical Center, Rotterdam, The Netherlands.
4 Department of Medical Statistics, Leiden University Medical Center, Leiden, The Netherlands.
5 Mathematical Institute Leiden University, Leiden, The Netherlands.
6 Department of Clinical Genetics, Academic Medical Center, Amsterdam, The Netherlands.
7 Bartiméus, Diagnostic Centre for Complex Visual Disorders, Zeist, The Netherlands.
8 Department of Human Genetics and Donders Institute for Brain, Cognition and Behaviour, Radboud University Medical Center, Nijmegen, The Netherlands.
9 Wilmer Eye Institute, Johns Hopkins University, Baltimore, Maryland, The United States of America.
10 Department of Epidemiology, Erasmus Medical Center, Rotterdam, The Netherlands.
11 Department of Ophthalmology, Radboud University Medical Center, Nijmegen, The Netherlands.
12 Rotterdam Eye Hospital, Rotterdam, The Netherlands.
13 The Netherlands Institute for Neuroscience (NIN-KNAW), Amsterdam, The Netherlands.

ABSTRACT

Purpose: To describe the phenotype and clinical course of patients with *RPGR*-associated retinal dystrophies, and to identify genotype-phenotype correlations.

Methods: A multicenter medical records review of 74 male patients with *RPGR*-associated retinal dystrophies.

Results: Patients had retinitis pigmentosa (RP; n = 52; 70%), cone dystrophy (COD; n = 5; 7%), or cone-rod dystrophy (CORD; n = 17; 23%). The median follow-up time was 11.6 years (range 0-57.1). The median age at symptom onset was 5.0 years (range 0-14 years) for patients with RP and 23.0 years (range 0-60 years) for patients with COD/CORD. The probability of being blind (best-corrected visual acuity <0.05) at the age of 40 was 20% and 55% in patients with RP and COD/CORD, respectively. *RPGR*-ORF15 mutations were associated with high myopia ($p = 0.01$), which led to a faster best-corrected visual acuity decline in patients with RP ($p < 0.001$) and COD/CORD ($p = 0.03$). Patients with RP with *RPGR*-ORF15 mutations had a faster visual field decline ($p = 0.01$) and thinner central retina ($p = 0.03$) than patients with mutations in exon 1 to 14.

Conclusion: Based on best-corrected visual acuity survival probabilities, the intervention window for gene therapy for *RPGR*-associated retinal dystrophies is relatively broad in patients with RP. *RPGR*-ORF15 mutations were associated with COD/CORD and with a more severe phenotype in RP. High myopia is a risk factor for faster best-corrected visual acuity decline.

INTRODUCTION

Pathogenic variants in the *RPGR* gene account for 70% to 80% of X-linked retinitis pigmentosa (RP) cases,[1, 2] and have also been described in rare cases of syndromic RP.[3] X-linked RP is one of the most severe forms of RP. Affected male patients typically start experiencing night blindness in childhood, with ensuing visual field restriction, and they have been described to reach blindness typically in the fourth or fifth decade of life.[4, 5] Mutations in the *RPGR* gene are also an important cause of cone dystrophy (COD) and cone-rod dystrophy (CORD).[2, 6]

X-linked COD and CORD are progressive diseases primarily affecting cones. The age at symptom onset of X-linked COD/CORD ranges between the second and fourth decade of life, and patients typically experience loss of visual acuity and color vision, photophobia, and central visual field defects,[7, 8] followed by rod dysfunction early in the disease course in X-linked CORD.[6] More than 300 different mutations in the *RPGR* gene have been identified,[9] with most mutations located in the guanine-cytosine-rich mutational hotspot ORF15.[10] Some studies have suggested genotype-phenotype correlations, showing a relatively more severe X-linked RP phenotype in patients with mutations in exon 1 to 14 than in patients with ORF15 mutations,[4, 11-13] whereas the opposite has also been observed, with a milder phenotype in patients with a mutation in exon 1 to 14 than in patients with ORF15 mutations.[14] So far, all the reported mutations in patients with X-linked COD/CORD have been found in the ORF15 region.[6, 15, 16] Mutations located toward the 3' end of ORF15 seem to be more often associated with predominant cone disease,[8, 16, 17] whereas mutations located toward the 5' end are more often found in RP.

Although no approved and effective treatment is clinically available for *RPGR*-related retinal dystrophies, functional and structural improvement has recently been shown after gene therapy in a canine *RPGR*-XLRP model,[18] and the first human gene therapy trial for *RPGR*-associated retinal dystrophies has started recently.[19] This promising progress in the development of human gene therapy for *RPGR*-associated retinal dystrophies necessitates an optimal insight in the natural disease course, which will help in the determination of the optimal therapeutic intervention window and in the identification of patients who are most likely to benefit from such treatments.

The aim of this study is to investigate the spectrum of phenotypes and the longitudinal clinical characteristics after long-term follow-up of a large cohort of patients with *RPGR*-related retinal dystrophies in the Netherlands.

MATERIALS AND METHODS

Study population

This study identified male patients with disease-causing variants in *RPGR* who underwent at least one clinical examination. Inclusion criteria were the following: a likely disease-causing variant in *RPGR* or a clinical diagnosis of an inherited retinal dystrophy, and a first- or second-degree relative with a likely disease-causing variant. We identified 96 male patients with *RPGR*-related retinal dystrophies. Of these patients, we excluded 22 male patients from further analyses, because they were from a large Dutch pedigree that was previously described,[7] and no additional follow-up data of these patients could be retrieved. Four male patients from that family had additional follow-up data and were included in our analyses.

Patients were collected from the patient database ("Delleman database") for genetic eye diseases at the Netherlands Institute for Neuroscience and Academic Medical Center (AMC) in Amsterdam,[20] and from various Dutch medical centers within the framework of the RD5000 consortium,[21] a Dutch registry of patients with retinal dystrophies. The study was approved by the Medical Ethics Committee of the Erasmus Medical Center and adhered to the tenets of the Declaration of Helsinki. Patients and/or their legal guardians signed informed consent forms for the use of their clinical data for research purposes.

Genetic analysis

Of the 74 male patients, 71 had received genetic mutational confirmation of their disease through direct Sanger sequencing (n = 52) or linkage analysis (n = 19) according to established protocols. DNA analysis was assisted by the CodonCode software (CodonCode Co). Three patients had not undergone genetic analysis but were affected first-degree relatives of a patient who had received genetic confirmation of an *RPGR* mutation. Mutational analyses were performed at the DNA diagnostics centers of Academic Medical Center (AMC) in Amsterdam, the Netherlands, or Radboud University Medical Center in Nijmegen, the Netherlands. Disease-causing variants in exon 16 to 19 were not detected in our set of 74 patients.

Clinical data collection

Data were obtained through standardized review of medical records for medical history, age at symptom onset and diagnosis, initial symptoms, visual acuity, refractive error, biomicroscopy of the anterior segment, dilated fundus examination, fundus photography, full-field electroretinography (ERG), Goldmann visual fields, spectral-domain optical coherence tomography (SD-OCT), and fundus autofluorescence (FAF) images (see Table, Supplemental Digital Content 1, which presents the data we were able to collect for this cohort).

Age at onset of disease was defined as the age at which the first symptom was noticed by the patient or the patients' parents in case of onset in infancy or early childhood. When symptoms were reported to have always been present, the age at onset was considered to be the first year of life.

Retinal cross sections and retinal thickness measurements were obtained with OCT. Most OCT data were obtained with Topcon (3D OCT-1000; Topcon Medical Systems, Tokyo, Japan) or Heidelberg Spectralis (Heidelberg Engineering, Heidelberg, Germany).
Goldmann visual field areas of the V4e target were digitized and converted to seeing retinal areas in mm^2, using a method described by Dagnelie.[22]

Statistical analysis
For statistical analysis, patients were stratified by predominant disease pattern: predominantly rod disease (RP), and predominant cone dystrophy (COD), defined as cone dysfunction without rod dysfunction on full-field ERG at the time of first evaluation, or cone-rod dystrophy (CORD), defined as both cone and rod dysfunction on full-field ERG, with relatively worse cone function. In most patients, full-field ERG was made only once, for diagnostic purposes, and therefore, ERG data could not be used for follow-up. In patients who were not examined by ERG, the diagnosis was made on clinical grounds. Categorical variables were expressed as proportions and continuous variables as mean values with SDs and medians with interquartile ranges (IQRs). To study the disease progression, a multistate model was estimated,[23] using the following states of visual impairment in the better-seeing eye: low vision (best-corrected visual acuity [BCVA] <20/67 and ≥20/200), severe visual impairment (BCVA <20/200 and ≥20/400), and blindness (BCVA <20/400), according to World Health Organisation criteria.[24] Linear mixed-model analysis was used to evaluate the annual decline rate of the seeing retinal area and of visual acuity, converting Snellen or decimal visual acuities to logMAR and using the better-seeing eye. We repeated this analysis for the worse-seeing eye to assess symmetry in BCVA decline rate. We used the values 2.7 for hand motion, 2.8 for light perception, and 2.9 for no light perception. We controlled for mutation location (ORF15 or exon 1 to 14), extent of myopia, defining high myopia as a spherical equivalent of the refractive error of more than -6 diopters (D),[25] moderate myopia as a spherical equivalent of the refractive error of more than -3D and ≤-6D, and mild myopia as a spherical equivalent of the refractive error of more than -0.75D and ≤-3D, and we stratified by diagnosis.

Asymmetry in visual acuity between two eyes was defined as a difference of ≥0.3 logMar (≥15 Early Treatment Diabetic Retinopathy Study letters), which is the threshold for clinical significance for changes in BCVA,[26] at two consecutive examinations or, in cases where only one BCVA measurement was available, the only examination. Data were analyzed using SPSS version 23.0 (IBM Corp). The multistate analysis was performed in the R software environment, version 3.3.1.[27]

RESULTS

Seventy-four patients from 39 families were investigated. Fifty-two patients (70%) had an RP phenotype, 17/74 (23%) had a CORD, 5/74 (7%) had a COD. Seventy patients (95%) were whites, three patients (4%) were blacks, and one patient (1%) was Asian.

Genetic analysis yielded 31 distinct pathogenic variants in the *RPGR* gene (see Table, Supplemental Digital Content 2, which further specifies these variants): 9 variants in exon 1 to 14 (20 patients, 27%) and 22 variants in exon ORF15 (54 patients, 73%). Of these variants, 24 (77% of all mutations) were frameshift mutations, one (3%) was a missense mutation, 4 (13%) were nonsense mutations, and 2 (6%) were splice-site mutations. The mutation type was not associated with the type of dystrophy (p = 0.8), but mutations in ORF15 were found in higher proportions (p = 0.005) in patients with COD/CORD (21/22, 95%) than in patients with RP (33/52, 63%). For the whole cohort, the median follow-up time was 11.6 years (IQR 18.4; range 0.0-57.1 years), with a median number of 5 visits per patient (IQR 7, range 1-55). The baseline characteristics of the patients in this study are shown in Table 1.

Disease onset and visual acuity

Data on the age at onset of symptoms were available for 25/51 (49%) patients with RP and 19/23 (83%) patients COD/CORD. When age at onset of the first symptom was not available, the age at diagnosis was used for analysis. The median age at symptom onset was 5.0 years (IQR 7.0; mean 5.2; range 0 [infancy]-14.0 years) in patients with RP and 23.0 years (IQR 39.0; mean 24.7; range 0-60.0 years) for patients with COD/CORD. Although the range in age at onset was high for patients with COD/CORD, patients within the same family reported an age at initial onset within the same decade of life, with the exception of 3 families. In one family, 2 brothers reported the same loss of subjective visual acuity, starting at the age of 35 in one brother, at the age of 60 in the other brother, and a grandson with visual acuity loss in the first decade of life, first noticed by the parents. In 2 other families, the large difference of 2 to 3 decades in age at first reported symptom was intergenerational, with an earlier recognition in the younger generation. The reported initial symptoms are specified in Table 1.

In 2/39 (5%) families, one harbouring a deletion after exon 10 and the other a truncating mutation relatively downstream in the ORF15 region of the *RPGR* gene, both RP and CORD phenotypes were reported in different patients within the same family. The prevalence of reported asthma and bronchitis was similar to the prevalence in the general Dutch population (Table 1).[28] BCVA data were available for 70/74 (95%) patients. Curves showing the probability of being in a state of low vision, severe visual impairment, or blindness, based on BCVA, are shown in Figure 1. For patients with RP, an ORF15 mutation signified a significantly higher yearly risk of reaching low vision than

a mutation in exon 1 to 14 (hazard ratio 2.2; 95% CI 0.8-6.1), and a higher yearly risk of becoming severely visually impaired after reaching low vision (hazard ratio 5.8; 95% CI 1.2-28.9).

For patients with RP, linear mixed models showed the age effect on BCVA decline to be 0.015 (3.5%) and 0.022 (5.3%) logMAR per year for patients with mutations in exon 1 to 14 ($p < 0.001$) and in ORF15 ($p < 0.0001$), respectively, which did not differ significantly from each other ($p = 0.11$). Considering the high proportion of patients with moderate or high myopia in this cohort, we assessed in patients with RP whether the extent of myopia significantly changed the BCVA decline rate compared to patients with emmetropia or hyperopia. In patients with RP, this was only the case for high myopia ($p = 0.003$) and not for mild ($p = 0.67$) or moderate myopia ($p = 0.58$). Patients with RP with high myopia had a BCVA decline rate of 0.032 logMAR (7.9%) per year ($p < 0.00001$), which was significantly faster ($p < 0.001$) than in patients with a refractive error less negative than -6D, where the BCVA decline was 0.013 logMAR (3.1%) per year. These rates were not significantly different between patients with mutations in exon 1 to 14 versus ORF15 ($p = 0.64$).

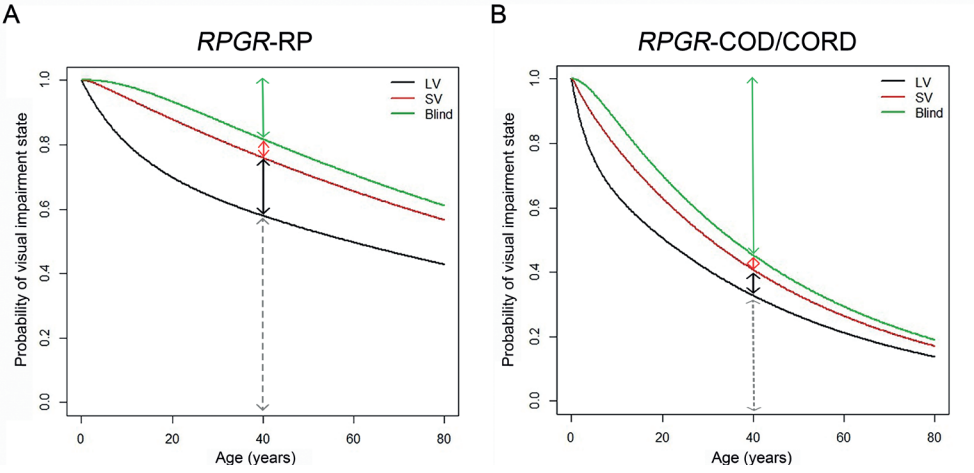

Figure 1. Multistate model-based disease progression curves showing the probability of being in a state of no visual impairment (BCVA ≥20/67), low vision (LV, BCVA <20/67 and ≥20/200), severe visual impairment (SV, BCVA <20/200 and ≥20/400), and blindness (BCVA <20/400) in the better-seeing eye in patients with RP (**A**) and patients with COD/CORD (**B**). The distances between the lines indicate the probability of being in a certain state at any age. The distance between 1) the 0% mark and the black line indicates the probability of not having low vision yet; 2) between the black and red line indicates the probability of having low vision; 3) between the red and green line indicates the probability of being severely visually impaired; 4) between the green line and the 100% mark indicates the probability of being blind. (Left panel) Patients with RP at the age of 40 had a 58% probability of not being visually impaired, a 17% probability of having low vision, a 7% probability of being severely visually impaired, and an 18% probability of being blind. They had a 50% probability of not being visually impaired at the age of 58. (Right panel) Patients with COD/CORD at the age of 40 had a 35% probability of not being visually impaired, a 10% probability of having low vision, a 5% probability of being severely visually impaired, and a 55% probability of being blind.

Performing this analysis for the BCVA decline of the worse-seeing eye yielded decline rates of 0.053 (12.9%) and 0.022 (5.3%) logMAR per year for patients with and without high myopia, respectively. Spline mixed models, used to explore rate (β) changes after a certain age, revealed faster BCVA decline rates at later decades of life in patients with RP, whereas before the age of 20, the BCVA in the overall RP group did not decline.

For patients with COD/CORD, like in RP, a significant overall age effect ($p < 0.0001$) on BCVA decline was seen, with a yearly decline of 0.023 logMAR or 5.5% in the better-seeing eye and 0.033 logMAR or 7.9% in the worse-seeing eye. The presence of high myopia was associated with a significantly faster BCVA decline ($p = 0.03$). A spline mixed model revealed a significantly faster BCVA decline of 0.038 (9.2%) logMAR per year in the better-seeing eye after 50 years of age, as compared to 0.019 (4.5%) logMAR per year before the age of 50 ($p < 0.001$). This same analysis did not reveal a significant change in slope of BCVA decline before and after the age of 20 ($p = 0.74$), 30 ($p = 0.89$), and 40 ($p = 0.72$) years in patients with COD/CORD. We found no significant differences in slope of decline before and after reaching low vision ($p = 0.32$ for COD/CORD; $p = 0.68$ for RP) and severe visual impairment ($p = 0.16$ for COD/CORD; $p = 0.24$ for RP).

Asymmetry in BCVA between eyes at the last 2 consecutive examinations was found in 11/48 (23%) patients with RP and 4/22 (18%) patients with COD/CORD. The presumed cause of asymmetry could be determined in 6/11 (55%) patients with RP and in 2/4 (60%) patients with COD/CORD (See Table, Supplemental Digital Content 3).

Ophthalmic and funduscopic findings

Myopia was present in 36/43 (84%) patients with RP and 17/20 (85%) patients with COD/CORD with available refractive error measurements. Patients became significantly more myopic with advancing age in the RP group (-0.07 D per year; $p < 0.001$) and the COD/CORD group (-0.09 D per year; $p = 0.014$). Based on the last available spherical equivalent, averaged between eyes, patients with an ORF15 mutation were significantly more myopic (mean -6.3 D; SD 3.9; range -14.1 D to +1.2 D) than patients with a mutation in exon 1 to 14 (mean -2.8 D; SD 3.5; range -7.9 D to +5.1 D; $p = 0.001$), and high myopia was found in a higher frequency than in patients with mutations in exon 1 to 14 ($p = 0.01$, chi-square test). The extent of myopia and other ophthalmic findings are shown in Table 1. Cataract or a history of cataract was reported in 26/43 (60%) patients with RP and 7/21 (33%) patients with COD/CORD with known lens status. In these patients, the median age at which cataracts were first reported was 33.3 years (n = 21; IQR 12.4; range 18.4-55.5 years) in patients with RP and was significantly earlier ($p < 0.001$, Mann-Whitney *U* test) than in patients with COD/CORD (n = 7; median 58; IQR 19; range 54-78 years).

Table 1. Cohort characteristics of *RPGR*-associated retinal dystrophies

Characteristics	Group total (n = 74)	RP (n = 52)	COD/CORD (n = 22)
Mean age at last exam ± SD (range), yrs	41.1 ± 20.2 (3.9-88.3)	39.3 ± 18.1 (9.2-77.5)	45.2 ± 24.3 (3.9-88.3)
Mean follow-up time ± SD, yrs	13.9 ± 13.2	13.8 ± 13.1	14.1 ± 13.7
Median follow-up time (range; IQR)	11.6 (0.0-57.1; 18.4)	10.9 (0.0-54.0; 19.8)	12.7 (0.0-57.1; 17.4)
Median number of visits (range; IQR)	5 (1-55; 7)	5 (1-22; 7)	5 (1-55; 5)
Mean number of visits ± SD	7.1 ± 7.7	6.6 ± 5.9	8.2 ± 11.0
Caucasian, n (%)	70 (95)	48 (92)	22 (100)
Asthma or bronchitis	7 (9)	5 (10)	2 (9)
Nystagmus or roving eye movements, n (%)	9 (12)	8 (16)*	1 (4)
Photophobia, n (%)	30 (41)	10/16 (63)	10/14 (71)
Reported first symptom, n (%)	45 (61)	25 (48)	20 (91)
Nyctalopia, n (%)	20 (44)	18 (72)	1 (5)
Visual field loss, n (%)	2 (4)	2 (8)	-
Photophobia, n (%)	1 (2)	-	1 (5)
Visual acuity loss, n (%)	18 (40)	3 (12)	17 (85)
Unknown, diagnosis used, n (%)	3 (7)	2 (8)	1 (5)
No symptom yet, n (%)	1 (2)	-	-
Mean refractive error ± SD (range)† (SER; n = 65), D	-5.3 ± 4.1 (-14.1 to +5.1)	-4.9 ± 3.9 (-13.0 to +5.1)	-6.3 ± 4.5 (-14.1 to +4.0)
High myopia (<-6D), n (%)	24 (38)	16/45 (36)	10/20 (50)
Moderate myopia (-3D > SER ≥ -6D), n (%)	21 (33)	16/45 (36)	7/20 (35)
Mild myopia (-0.75D > SER ≥ -3D), n (%)	8 (13)	7/45 (16)	1/20 (5)
≥-0.75D, n (%)	10 (16)	6/45 (13)	2/20 (10)
Fundoscopic examination			
Optic disc pallor, n (%)	50/60 (83)	39/40 (98)	11/20 (55)
Peripapillary atrophy, n (%)	15/60 (25)	9/40 (23)	6/20 (30)
Bone-spicule or coarse hyperpigmentation, n (%)	44/58 (76)	37/42 (88)	7/16 (44)
Vascular attenuation, n (%)	52/63 (81)	43/44 (98)	10/19 (53)
Macular phenotype described, n (%)	55 (74)	34 (65)	21 (95)

Table 1. Continued

No macular RPE changes	7/55 (13)	4/34 (12)	3/21 (14)
RPE atrophy with relative foveal sparing, resembling bull's eye maculopathy, n (%)	10/55 (18)	6/34 (18)	4/21 (19)
Other form of RPE atrophy, n (%)	24/55 (44)	13/34 (38)	10/21 (48)
Alterations, no profound atrophy, n (%)	14/55 (25)	11/34 (32)	4/21 (19)
Electroretinography pattern last seen, n (%)	48 (65)	30 (58)	18 (82)
Scotopic and photopic ND, n (%)	22/48 (46)	21/30 (70)	1/18 (6)
Rod-cone pattern, n (%)	6/48 (13)	6/30 (20)	-
Cone-rod pattern, n (%)	11/48 (23)	-	11/18 (61)
Cone isolated, n (%)	3/48 (6)	-	3/18 (17)
Scotopic and photopic reduced, pattern not further specified, n (%)	5/48 (10)	3/30 (10)	2/18 (11)
Normal, n (%)	1/48 (2)	-	1/18 (6)

* One of these patients had nystagmus after a head trauma.

† Mean spherical equivalent of the right eye and the left eye. If patients had undergone cataract surgery, the last SER before surgery was used.

ND, nondetectable amplitudes; SER, spherical equivalent of the refractive error.

Table 1 shows the funduscopic findings in this cohort. Retinal pigment epithelium changes in the macula were found in all but 3 patients with RP aged 17, 20, and 31 and in all but 4 patients with COD/CORD aged 3 to 10 at the time of the last funduscopic examination. Optic disc drusen were found in 5/52 (10%) patients with RP and not in patients with COD/CORD. A tapetal reflex was reported in one RP patient (2%) at the age of 20, and in 2/23 (9%) patients with COD/CORD, at the ages of 9 and 39. White drusen-like deposits were found in the (mid-) peripheral retina in 4/51 (8%) patients with RP (see Figure, Supplemental Digital Content 4, showing fundus photographs for *RPGR*-RP), in the peripheral macula in one patient with COD, and in the peripheral retina in one patient with CORD (see Figure, Supplemental Digital Content 5, showing fundus photographs for *RPGR*-COD/CORD).

In 10 patients, a history of uncomplicated cataract surgery at the median age of 46 in patients with RP (n = 7; IQR 40; range 29-69) and at the median age of 66 in patients with COD/CORD (n = 3; ages 64, 66, and 79 years), due to visually significant cataract, was documented.

Full-field ERG and visual field findings

Electroretinography was available for 30/52 (58%) patients with RP and 18/22 (82%) patients with COD/CORD. For patients with RP, the median age at which cone and rod ERG amplitudes were first found to be nondetectable, was 17.4 years (IQR 24.0; range 5.3-40.6 years; mean 22.4 years; SD 12.5). Of the 21 patients with RP with a nondetectable ERG, 6 had previously documented recordable cone (6/6) and rod (3/6) ERG responses. The median age at this last-documented ERG response before progressing to a nondetectable ERG was 12.6 years (IQR 24.5, range 4.7-30.5 years).

In patients with COD/CORD, only one patient had a nondetectable cone and rod ERG at the age of 35.1 years, with the last documented recordable but attenuated cone and rod ERG response at 9 years of age. One 4-year-old patient from a large CORD pedigree had a normal ERG, in the presence of suboptimal BCVA and a mild color vision deficiency as measured with Ishihara plates, and no clear fundus abnormalities. The ERG patterns are further specified in Table 1. Progression of ERG from an isolated COD pattern to a CORD pattern was not documented in this cohort, but all patients with COD/CORD only received one (56%) or 2 (44%) ERGs during the observational period.

Goldmann visual fields were available for 25/52 (48%) patients with RP and 6/22 (27%) patients with COD/CORD, and within individuals with follow-up Goldmann visual fields (n = 11; 9 patients with RP and 2 patients with COD/CORD), the median follow-up time was 11.0 years (IQR 11.9; range 2.0-35.9 years; see Figure, Supplemental Digital Content 6, which shows the individual visual field areas). Linear mixed-model analysis of the age effect on logarithm of the seeing retinal areas revealed a significantly faster Goldmann visual field decline in patients with RP than in patients COD/CORD patients ($p = 0.001$), with a yearly decline in seeing retinal area of 6.6% ($p < 0.0001$) in the overall RP population. Significant differences in baseline seeing retinal area were seen between individual patients with COD/CORD ($p = 0.001$), and no significant overall age effect in patients with COD/CORD ($p = 0.26$) was found. However, in patients with COD/CORD, there was a yearly decline rate of 2.1% in seeing retinal area after the age of 40 that was significantly faster ($p = 0.02$) than before the age of 40.

In patients with RP, the logarithm of the seeing retinal area size was significantly smaller at baseline in patients with mutations in exon 1 to 14 than in patients with mutations in ORF15 ($p = 0.05$) of *RPGR*, but declined significantly faster ($p = 0.014$) in patients with a mutation in the ORF15

region, with a yearly decline rate of 9.0% ($p < 0.00001$), as compared to 4.2% in patients with mutations in exon 1 to 14 ($p = 0.004$).

Findings on retinal imaging in *RPGR*-associated retinitis pigmentosa

Fundus autofluorescence images were available for 17/52 (33%) patients with RP, and general age-related changes are further specified in Table 2. A hyperautofluorescent ring was found in 8/17 (47%) patients with RP, all under the age of 22 and with a BCVA ≥0.5 in both eyes (Figure 2). In patients with a hyperautofluorescent ring and available concurrent SD-OCT scans (n = 5), this ring demarcated a relatively preserved macula on OCT (Figure 2), and the ring represented a transition from a relatively preserved outer retina to a more degenerated outer retina on SD-OCT. Larger ring diameters were found in younger patients, with the largest ring diameter spanning the posterior pole in a 9-year-old patient, and the smallest ring diameter in the oldest patient.

Optical coherence tomography data were available for 15/52 (29%) patients with RP with a mean age of 28.1 years (SD 14.8, range 13.2-67.2 years). No patients with RP had documented cystoid fluid collections in the macula at any time point in the follow-up period, and 6/15 (40%) had some degree of eccentric or parafoveal macular epiretinal membrane in at least one eye (Figure 2D).

Central retinal thickness (CRT) measurements with Heidelberg SD-OCT were available for 14/52 (27%) patients with RP. Mixed-model analysis of longitudinal and cross-sectional CRT data revealed a significant age effect on CRT (-3 μm/year; $p = 0.004$). *RPGR* mutations in exon 1 to 14 were associated with a significantly thicker CRT than mutations in the ORF15 region ($p = 0.03$). The median of the last-measured CRT was 244 μm (IQR 102; range 102-265 μm) in exon 1 to 14 and 147 μm (IQR 61; range 88-227 μm) in ORF15, with similar ages between both groups. Data on the structural integrity of the foveal and peripheral macular ellipsoid zone (EZ) and outer nuclear layer (ONL) are specified in Table 2.

Table 2. Imaging findings in patients with *RPGR*-associated retinal dystrophies

Retinitis pigmentosa			N (%)	Age (years)
FAF	No FAF abnormalities or only a hyper-AF ring around the macula		3/17 (18)	12-16
	Granular/mottled hypo-AF changes, more abundant outside the vascular arcade than in the posterior pole		9/17 (53)	9-30
	Marked FAF decrease in periphery, with some remnants of FAF in the posterior pole		3/17 (18)	36-45
	Near-complete absence of FAF in the whole retina		2/17 (12)	68-70
	Structural integrity on SD-OCT		N (%)	Age (years)
EZ	Central macula	Peripheral macula		
	Intact	Intact	3/12 (25)	14-19
	Intact	Granular/attenuated	4/12 (33)	16-31
	Attenuated, relatively spared	Almost absent	4/12 (33)	27-45
	Not visible	Not visible	1/12 (8)	67
ONL	Intact	Intact	3/12 (25)	16-19
	Intact/relatively spared	Attenuated	3/12 (25)	14-31
	Atrophic	Atrophic	5/12 (42)	27-45
	Nearly absent	Nearly absent	1/12 (8)	67
Cone/cone-rod dystrophy			N (%)	Age (years)
FAF	No FAF abnormalities*		1/11 (9)	3
	Only hyper-AF ring, no FAF abnormalities in- or outside ring		2/11 (18)	18-31
	Central FAF decrease with or without a hyper-AF ring, surrounded by (nearly) normal FAF		5/11 (45)	38-63
	Central FAF decrease and a hyper-AF ring, surrounded by mild patchy hypo-AF changes		1/11 (9)	11
	Central FAF absence, surrounded by a hyper-AF border; paravascular satellite lesions of absent autofluorescence		1/11 (9)	79
	Granular AZOOR-like changes		1/11 (9)	67
	Structural integrity on SD-OCT		N (%)	Age (years)
EZ	Central macula	Peripheral macula		
	Intact	Intact	4/10 (40)	3-19
	Interrupted	Intact	5/10 (50)	37-67
	Nearly absent	Granular/interrupted	1/10 (10)	79
ONL	Intact	Intact	3/10 (30)	3-19
	Atrophic	Intact	3/10 (30)	40-59
	Atrophic†	Atrophic	3/10 (30)	31-79
	Intact	Atrophic	1/10 (10)	18

* Because of the very young patient age, the picture quality was relatively low and did not allow for reliable visualization outside of the posterior pole.

† Atrophy of the foveal ONL in cone/cone-rod dystrophy patients was always more marked than the atrophy of the ONL outside of the central macula.

AZOOR, acute zonal occult outer retinopathy.

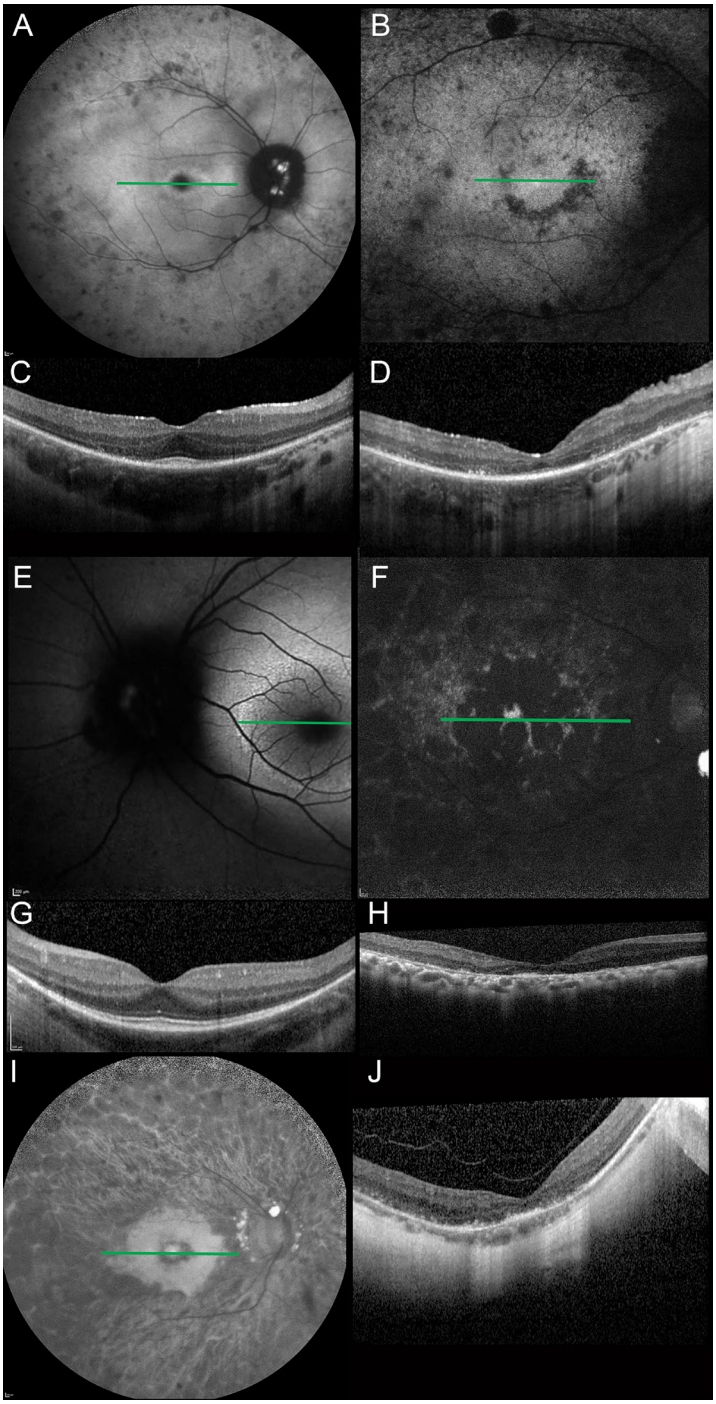

Figure 2. Findings on imaging in patients with *RPGR*-associated retinitis pigmentosa. The green lines in the FAF images show the location of the complementary SD-OCT scans. **A.** Fundus autofluorescence image of a 19-year-

old patient with a missense mutation in exon 5 (c.425T>G; p.(Ile142Ser); BCVA in the right eye 20/25; in the left eye 20/20), showing optic disc drusen, a small hyperautofluorescent ring around the central macula, surrounded by patchy regions of decreased autofluorescence (AF). **B.** Fundus autofluorescence image of a 28-year-old patient with a frameshift mutation (c.2362_2366del; p.(Glu788Argfs*45)) in *RPGR*-ORF15 (BCVA in the right eye 20/50; in the left eye 20/67), showing dense granular areas of decreased AF around the optic disc, vascular arcade, and in the posterior pole, with a hypo-AF border around the central macula. **C.** Spectral domain OCT of the same patient in (**A**), showing central sparing of the EZ, external limiting membrane (ELM), and ONL, whereas these layers are attenuated toward the peripheral macula. **D.** Spectral domain OCT of the same patient described in (**B**), showing an epiretinal membrane, and atrophic EZ, ELM, and ONL, with a granular aspect of the EZ, but with relative central sparing. **E.** Fundus autofluorescence image of a 16-year-old patient with a missense mutation in exon 5 (BCVA in both eyes 20/20), showing a hyper-AF ring. **F.** Fundus autofluorescence image of a 45-year-old patient with a pathogenic frameshift mutation (c.2405_2406del; p.(Glu802Glyfs*32)) in *RPGR*-ORF15 (BCVA in the right eye 20/125; in the left eye 20/400), showing markedly decreased patchy AF with scattered granular remnants of hyper-AF. **G.** Spectral domain OCT of the same patient described in (**E**), showing a wide sparing of the EZ, ELM and ONL, but with attenuation in the peripheral macula. **H.** Spectral domain OCT of the same patient in (**F**), showing markedly attenuated EZ, ELM, and ONL in the macula, more so in the peripheral macula. **I.** Fundus autofluorescence image of a 42-year-old patient with a pathogenic frameshift mutation (c.27del; p.(Asp10Ilefs*58)) in exon 1 (BCVA in both eyes 20/63), showing generally decreased AF, papillary drusen, and a hyper-AF fovea, encircled by a hypo-AF ring, surrounded by a region of hyper-AF. Foveal hyperautofluorescence, surrounded by hypo-autofluorescence in varying intensities, was found in 3/15 (20%) patients with RP, aged 28 years to 42 years and with a BCVA between 20/100 and 20/50. **J.** Spectral domain OCT of the same patient described in (**I**), showing atrophy of the ONL. The EZ has a granular aspect in the fovea, and is almost absent outside of the fovea.

Findings on retinal imaging in *RPGR*-associated cone dystrophy/cone-rod dystrophy

Fundus autofluorescence images were available for 11/22 (50%) patients with COD/CORD, and generally showed a hyperautofluorescent ring around a hypo-autofluorescent macula (7/11, 64%) (Figure 3). Further details are given in Table 2. In patients with COD/CORDwith a hyperautofluorescent ring and a concurrent SD-OCT scan (n = 4), this ring demarcated an area of a relatively atrophic macula in 3 patients aged 38 to 79, which was essentially the opposite pattern as compared to the RP group, with marked attenuation of the external limiting membrane, the ellipsoid zone (EZ), and the retinal pigment epithelium centrally within the hyperautofluorescent ring (Figure 3). Only in the youngest patient with CORD, aged 18, who had a double concentric hyperautofluorescent ring, the inner ring demarcated an area of relatively healthy EZ, external limiting membrane, and ONL (Figure 3, A and B). We did not observe a consistent relation between hyperautofluorescent ring diameter size and age.

Optical coherence tomography data were available for 12/22 (55%) patients with COD/CORD with a mean age of 41.8 years (SD 25.8, range 3.9-79.4 years). Cystoid fluid collections in both eyes were noted in 2/12 (17%), and 1/12 (8%) had a bilateral epiretinal membrane. Central retinal thickness measurements with Heidelberg SD-OCT were available for 10/22 (45%) patients. Mixed-model analysis of longitudinal and cross-sectional CRT data revealed a significant age effect on CRT (-2 μm/year; $p = 0.008$). Only 1/10 patients with CORD with SD-OCT had a mutation in

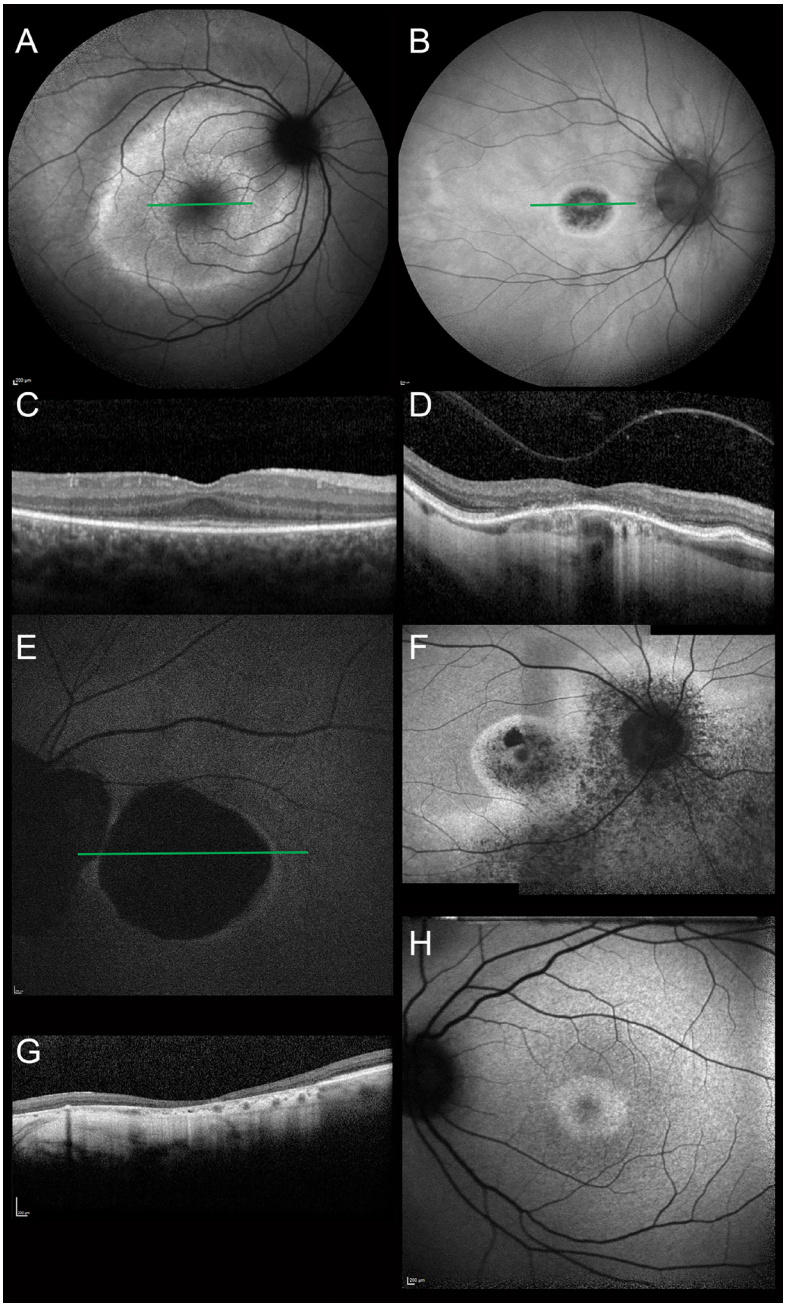

Figure 3. Findings on imaging in patients with *RPGR*-associated predominantly cone-involving dystrophies. The green lines in the FAF images show the location of the complementary SD-OCT scans. The retina around the hyperautofluorescent ring (in 8 patients) showed normal autofluorescence in 6/8 (75%) patients, whereas in the other 2 patients, this ring was surrounded by mild patchy hypo-autofluorescent changes in one patient, and by paravascular

satellite lesions of absent autofluorescence in another patient. **A.** Fundus autofluorescence image of an 18-year-old patient with a deletion after *RPGR* exon 10 (c.1246-?_*1091-?) and a CORD pattern on electroretinogram (BCVA in the right eye 20/67; in the left eye 20/40), showing a double concentric hyper-AF ring. **B.** Fundus autofluorescence image of a 54-year-old patient with a nonsense mutation (c.2959G>T; p.(Glu987*)) in *RPGR*-ORF15 (BCVA in the right eye 20/100; in the left eye 20/400), showing central hypo-AF with relatively preserved foveal AF, a hyper-AF ring, and normal surrounding retina. **C.** Spectral domain OCT scan of the same patient described in (**A**), showing relatively well-preserved EZ, ELM, and ONL in the central macula, with some attenuation toward the periphery. **D.** Spectral domain OCT of the same patient described in (**B**), showing a continuous EZ and ELM and a relatively healthy ONL in the peripheral retina, but attenuation of these layers in the central macula. The choroid is markedly thinned, mainly in the peripheral macula. **E.** Fundus autofluorescence image of a 79-year-old patient with a frameshift mutation in *RPGR*-ORF15 (c.3317dup; p.(Ser1107Valfs*4); BCVA in the right eye 20/400; in the left eye 2/100), showing peripapillary atrophy, a central absence of AF, surrounded by a thin border of slightly increased AF. **F.** Fundus autofluorescence image of a 67-year-old patient with a frameshift mutation (c.2993_2996del; p.(Glu998Glyfs*90)) in *RPGR*-ORF15 (BCVA in the right eye 20/40; in the left eye 20/50). This patient had bilateral granular hypo-AF and hyper-AF changes around the optic disc and in the central macula, encircled by an area of increased AF, and extending to the inferotemporal vessels and inferior retina, in an acute zonal occult outer retinopathy-like distribution, and a relatively preserved aspect of the fovea. No SD-OCT was available for this patient. **G.** Spectral domain OCT of the same patient described in (**E**), showing a markedly thinned neuroretina, retinal pigment epithelium, and choroid. **H.** Fundus autofluorescence image of a 31-year-old patient with a frameshift mutation (c.3039_3040del; p.(Glu1014fs)) in *RPGR*-ORF15 (BCVA in both eyes 20/33), showing a small but broad hyper-AF ring around the fovea. No SD-OCT scan was available for this patient.

the exon 1 to 14 region, and his CRT (247 μm, averaged between eyes) was higher than the CRT in patients with COD/CORD with ORF15 mutations (126 μm, range 93-173 μm). Data on the structural integrity of the foveal and peripheral macular EZ and ONL are depicted in Table 2.

DISCUSSION

is retrospective cohort study, we describe the natural disease history and phenotypic spectrum of *RPGR*-associated retinal dystrophies in 74 patients from 38 different families.

We found variability in the initial presentation. Phenotypic heterogeneity associated with a single mutation in the same family was seen in 2 families, each comprising 2 to 3 patients, pointing to a modest influence of genetic and/or environmental modifiers on the phenotype. Cases of RP and CORD within the same family carrying an identical *RPGR* mutation have been described previously,[11, 29, 30] and significant intrafamilial variability in the age at symptom onset and BCVA has been described within families with *RPGR*-associated RP.[31]

Most patients with RP in this cohort showed typical RP fundus features and macular involvement from the second decade of life onward. In patients with COD/CORD, a normal macula was only seen in the youngest patients up to 10 years of age.

The median age at symptom onset in patients with COD/CORD was 23 years in this cohort, with a wide range. This is more than 10 years earlier than reported previously in a single large *RPGR* family,[7] but 7 years to 11 years later than in a previously described genetically heterogeneous COD/CORD cohort.[32] However, the accuracy of self-reported age at symptom onset could not be ascertained in this retrospective study setting. Progression on full-field ERG from a COD pattern to a CORD pattern was not documented in this cohort, because ERG is used in the clinical setting for diagnostic rather than follow-up purposes. An earlier review described characteristic early secondary rod involvement in CORD, and no or possibly late rod involvement in COD, signifying considerable overlap between these two diagnoses and meaning that rod involvement in later life could still be concurrent with a COD diagnosis.[6]

In our study cohort, the rate of BCVA decline in patients with COD/CORD showed a significantly faster decline after the age of 50. A recent natural history study in patients with Stargardt disease found a significant association of baseline BCVA level with the yearly rate of BCVA change, as BCVA in eyes with moderate impairment declined faster than the BCVA in eyes with mild or no impairment, but slower than in eyes with severe impairment.[33] We did not observe this difference in this cohort of *RPGR*-associated COD/CORD and RP.

Imaging findings in this cohort included the presence of a hyperautofluorescent ring in 47% of patients with RP with available FAF imaging, with larger rings in younger patients, demarcating an area of relatively spared retina. In patients with COD/CORD with available FAF, a hyperautofluorescent ring was found in 73%, with larger rings in older patients, demarcating an area of relatively atrophic retina with EZ and ONL attenuation. In all patients, the hyperautofluorescent ring represented a transitional zone between relatively healthy and more severely affected retina. This further supports the earlier findings that larger rings in RP and smaller rings in COD/CORD indicate greater preservation of structure and function, with progressive ring size reduction indicating disease progression outside the ring in RP,[34-36] and progressive ring expansion indicating disease progression within the ring in COD/CORD.[8, 37] In this context, the implication of our finding of a double concentric ring in an 18-year-old patient with CORD with a relatively healthy fovea within the inner concentric ring is unclear. An earlier study of *NR2E3*-associated autosomal dominant RP found progressive centripetal and centrifugal degeneration in the area between both concentric rings, with the inner ring becoming progressively smaller, closing in on the healthy central macula, and the outer ring size expanding.[38] This pattern would explain the relatively healthy fovea in this patient with CORD, despite the cone-rod pattern on ERG. However, there was no SD-OCT available of the macular area colocalizing with the outer concentric ring that could support this hypothesis. Multifocal ERG would allow the measurement of localized retinal function, particularly the integrity of the central macular area. Longitudinal FAF imaging in a prospective setting is necessary to further assess whether the presence and size of a hyperautofluorescent ring can assist in identifying regions amenable to future gene therapy.

We found several genotype-phenotype correlations in this study. In summary, we found a potentially more deleterious effect of mutations in the ORF15 region of the *RPGR* gene than mutations in exon 1 to 14. First, patients with RP with a pathogenic *RPGR*-ORF15 variant had a significantly higher yearly hazard of reaching low vision and severe visual impairment. Next, patients with RP with ORF15 mutations had higher myopia, a significantly thinner central retina, and a significantly faster decline of the V4e seeing retinal area than patients with exon 1 to 14 mutations, with decline rates of 9.0% and 4.2%, respectively. By contrast, most studies in literature have reported a more severe phenotype in patients with exon 1 to 14 mutations, as defined by a faster loss of ERG amplitudes,[4, 12] or a smaller visual field.[13] Exceptions have been described, with a more severe phenotype in patients with mutations in ORF15,[14] and worse visual function even in female carriers of *RPGR*-ORF15.[39] To further complicate the picture, similar decline rates in BCVA and visual field have been described between patients with mutations in exon 1 to 14 and ORF15, despite a faster loss of ERG cone function in patients with mutations in exon 1 to 14.[4] Finally, a higher degree of phenotypic heterogeneity has been reported in patients with *RPGR*-ORF15 mutations than in patients with exon 1 to 14 mutations, which could in part explain the variable observations.[12, 29] In interpreting the novel associations in this study, it is judicious to consider the relatively small numbers of patients in subgroup analyses of the visual field data (n = 31) and SD-OCT data (n = 27), as compared to the BCVA (n = 70) and refractive error (n = 65) data. In addition, the interpretation of retrospective data is complicated by potential between-center and interexaminer variability, which may not always be statistically accounted for in the retrospective study setting. Although data gathered from clinical practice are useful, these findings warrant further investigation, in larger patient groups and in a controlled prospective setting.

So far, most of all previously reported cases of *RPGR*-associated COD/CORD have contained a mutation in the 3' end of the ORF15 region. By contrast, mutations toward the 5' end were associated with a higher RP frequency.[6, 8, 11, 15, 16] Patients with COD/CORD in our study generally had ORF15 mutations toward the 3' end, supporting these earlier findings, but we also report the first case of a predominantly cone-affecting dystrophy caused by a deletion after exon 10. This adds to the phenotypic heterogeneity in exon 1 to 14. This patient was member of a family with RP patients.

Regarding future (gene) therapeutic options, the visual acuity survival results in this retrospective study suggest a potentially broad intervention window for gene therapy in the first 6 decades of life in patients with RP, as we found a 50% probability of not being visually impaired (i.e., BCVA <20/67) at the age of 58, indicating relative preservation of foveal photoreceptors before this time. In patients with COD/CORD, the potential intervention window for gene therapy is narrower than in RP, although the wide range in symptom onset and high variability in clinical course warrants additional patient-by-patient eligibility assessment. The relatively fast BCVA decline rates in this cohort suggest that BCVA change may be a potentially sensitive outcome parameter of treatment in future therapeutic trials, particularly in patients with RP with increasing age and in patients

with COD/CORD after the age of 50. In patients with RP under the age of 20, BCVA may not be a sensitive measure to detect therapeutic effect. When assessing patient eligibility for a gene therapy trial, special attention to the presence of high myopia is warranted, as high myopia was prevalent in this RP and COD/CORD cohort, and was significantly associated with a faster annual BCVA decline, potentially due to additional myopic degeneration. Earlier studies have shown that, of all refractive errors, high myopia entails the highest risk of visual impairment.[40, 41] As retinal structure also needs to be assessed to determine the potential therapeutic intervention window, we found an intact foveal EZ on SD-OCT up until the fifth decade of life in patients with RP, although the EZ in the extrafoveal and more peripheral macula was attenuated from the second decade of life onward, indicating a progressive centripetal degeneration. Outer nuclear layer attenuation seemed to occur earlier, from the second decade of life onward, although detecting ONL thinning on SD-OCT may be easier than visualizing change in EZ intensity. This is an interesting observation nonetheless, as protein RPGR-ORF15 localizes to the connecting cilium of the photoreceptors and therefore probably the EZ on OCT. In a canine model with a naturally occurring *RPGR* mutation in the ORF15 region, severe photoreceptor outer segment disintegration preceded thickness reduction of the ONL, which only started to decline at older ages in the inferior retina, with preserved thickness in the visual streak.[42, 43] Another canine model with a naturally occurring *RPGR*-ORF15 mutation showed a more rapid ONL thickness decline, with the visual streak more severely affected than the periphery.[42]

In patients with COD/CORD in this cohort, the foveal EZ and ONL were only intact until the second decade of life and showed a granular appearance until the seventh decade of life in some patients, although in others the EZ was nearly absent from the sixth decade onward. *RPGR* gene therapy in a canine model has shown retinal functional and structural rescue in initial stage disease, that is, before ONL reduction, midstage disease, that is, 40% ONL loss, and late-stage disease, that is, 50% to 60% ONL loss, expanding the therapeutic window, although the time between subretinal injection and observed rescue increased with advancing disease stage. The relatively common occurrence of an epiretinal membrane may complicate the outcome of subretinal gene therapy surgery, possibly requiring removal of the epiretinal membrane before subretinal injection of the therapeutic vector.

This study suggests that the use of the contralateral eye as an untreated control in future therapeutic trials may be appropriate, as we found symmetry in BCVA between eyes in 77% of patients with RP and patients with COD/CORD, suggesting that *RPGR*-associated retinal dystrophies are commonly symmetrical between eyes in most patients. However, we did find a faster yearly BCVA decline rate in the worse eye than in the better eye. Asymmetry of structural progression on FAF and OCT in *RPGR*-associated RP has been described before.[35] So far, gene therapeutic trials have treated the worse-seeing eye and used the better-seeing eye as an untreated control.[44-47] In future clinical trials, it may be useful to include a retrospective comparison of the natural course of structural and functional decline between eyes of individual patients when assessing therapeutic effect.

REFERENCES

1. Shu X, Black GC, Rice JM, et al. RPGR mutation analysis and disease: an update. Hum Mutat 2007;28:322-328.
2. Pelletier V, Jambou M, Delphin N, et al. Comprehensive survey of mutations in RP2 and RPGR in patients affected with distinct retinal dystrophies: genotype-phenotype correlations and impact on genetic counseling. Hum Mutat 2007;28:81-91.
3. Zito I, Downes SM, Patel RJ, et al. RPGR mutation associated with retinitis pigmentosa, impaired hearing, and sinorespiratory infections. J Med Genet 2003;40:609-615.
4. Sandberg MA, Rosner B, Weigel-DiFranco C, et al. Disease course of patients with X-linked retinitis pigmentosa due to RPGR gene mutations. Invest Ophthalmol Vis Sci 2007;48:1298-1304.
5. Flaxel CJ, Jay M, Thiselton DL, et al. Difference between RP2 and RP3 phenotypes in X linked retinitis pigmentosa. Br J Ophthalmol 1999;83:1144-1148.
6. Michaelides M, Hardcastle AJ, Hunt DM, Moore AT. Progressive cone and cone-rod dystrophies: phenotypes and underlying molecular genetic basis. Surv Ophthalmol 2006;51:232-258.
7. Thiadens AA, Soerjoesing GG, Florijn RJ, et al. Clinical course of cone dystrophy caused by mutations in the RPGR gene. Graefes Arch Clin Exp Ophthalmol 2011;249:1527-1535.
8. Ebenezer ND, Michaelides M, Jenkins SA, et al. Identification of novel RPGR ORF15 mutations in X-linked progressive cone-rod dystrophy (XLCORD) families. Invest Ophthalmol Vis Sci 2005;46:1891-1898.
9. Shu X, McDowall E, Brown AF, Wright AF. The human retinitis pigmentosa GTPase regulator gene variant database. Hum Mutat 2008;29:605-608.
10. Vervoort R, Lennon A, Bird AC, et al. Mutational hot spot within a new RPGR exon in X-linked retinitis pigmentosa. Nat Genet 2000;25:462-466.
11. Yang L, Yin X, Feng L, et al. Novel mutations of RPGR in Chinese retinitis pigmentosa patients and the genotype-phenotype correlation. PLoS One 2014;9:e85752.
12. Fahim AT, Bowne SJ, Sullivan LS, et al. Allelic heterogeneity and genetic modifier loci contribute to clinical variation in males with X-linked retinitis pigmentosa due to RPGR mutations. PLoS One 2011;6:e23021.
13. Sharon D, Sandberg MA, Rabe VW, et al. RP2 and RPGR mutations and clinical correlations in patients with X-linked retinitis pigmentosa. Am J Hum Genet 2003;73:1131-1146.
14. Andreasson S, Breuer DK, Eksandh L, et al. Clinical studies of X-linked retinitis pigmentosa in three Swedish families with newly identified mutations in the RP2 and RPGR-ORF15 genes. Ophthalmic Genet 2003;24:215-223.
15. Branham K, Othman M, Brumm M, et al. Mutations in RPGR and RP2 account for 15% of males with simplex retinal degenerative disease. Invest Ophthalmol Vis Sci 2012;53:8232-8237.
16. Demirci FY, Rigatti BW, Wen G, et al. X-linked cone-rod dystrophy (locus COD1): identification of mutations in RPGR exon ORF15. Am J Hum Genet 2002;70:1049-1053.
17. Yang L, Wu L, Yin X, et al. Novel mutations of CRB1 in Chinese families presenting with retinal dystrophies. Mol Vis 2014;20:359-367.
18. Beltran WA, Cideciyan AV, Iwabe S, et al. Successful arrest of photoreceptor and vision loss expands the therapeutic window of retinal gene therapy to later stages of disease. Proc Natl Acad Sci U S A 2015;112:E5844-E5853.

19. New trial for Blindness Rewrites the Genetic Code. University of Oxford, 2017. Available at: http://www.ox.ac.uk/news/2017-03-17-new-trial-blindness-rewrites-genetic-code. Accessed May 2, 2017.
20. van den Born LI, Bergen AA, Bleeker-Wagemakers EM. A retrospective study of registered retinitis pigmentosa patients in The Netherlands. Ophthalmic Paediatr Genet 1992;13:227-236.
21. van Huet RA, Oomen CJ, Plomp AS, et al. The RD5000 database: facilitating clinical, genetic, and therapeutic studies on inherited retinal diseases. Invest Ophthalmol Vis Sci 2014;55:7355-7360.
22. Dagnelie G. Conversion of planimetric visual field data into solid angles and retinal areas. Clin Vis Sci 1990;5:95-100.
23. Putter H, Fiocco M, Geskus RB. Tutorial in biostatistics: competing risks and multi-state models. Stat Med 2007;26:2389-2430.
24. World Health Organization. International Statistical Classification of Diseases and Related Health Problems, 10th Revision (ICD-10). 2003. Available at: http://www.who.int/classifications/icd/en/. Accessed April 5, 2017.
25. Verhoeven VJ, Buitendijk GH, Rivadeneira F, et al. Education influences the role of genetics in myopia. Eur J Epidemiol 2013;28:973-980.
26. Csaky KG, Richman EA, Ferris IIIFL. Report from the NEI/FDA Ophthalmic Clinical Trial Design and Endpoints Symposium. Invest Ophthalmol Vis Sci 2008;49:479-489.
27. R Core Team. R: A Language and Environment for Statistical Computing. Vienna, Austria: R Foundation for Statistical Computing, 2013.
28. Cai Y, Zijlema WL, Doiron D, et al. Ambient air pollution, traffic noise and adult asthma prevalence: a BioSHaRE approach. Eur Respir J 2017;49.
29. Ruddle JB, Ebenezer ND, Kearns LS, et al. RPGR ORF15 genotype and clinical variability of retinal degeneration in an Australian population. Br J Ophthalmol 2009;93:1151-1154.
30. Walia S, Fishman GA, Swaroop A, et al. Discordant phenotypes in fraternal twins having an identical mutation in exon ORF15 of the RPGR gene. Arch Ophthalmol 2008;126:379-384.
31. Sheng X, Li Z, Zhang X, et al. A novel mutation in retinitis pigmentosa GTPase regulator gene with a distinctive retinitis pigmentosa phenotype in a Chinese family. Mol Vis 2010;16:1620-8.
32. Thiadens AA, Phan TM, Zekveld-Vroon RC, et al. Clinical course, genetic etiology, and visual outcome in cone and cone-rod dystrophy. Ophthalmology 2012;119:819-826.
33. Kong X, Strauss RW, Michaelides M, et al. Visual Acuity Loss and Associated Risk Factors in the Retrospective Progression of Stargardt Disease Study (ProgStar Report No. 2). Ophthalmology 2016;123:1887-1897.
34. Duncker T, Tabacaru MR, Lee W, et al. Comparison of near-infrared and short-wavelength autofluorescence in retinitis pigmentosa. Invest Ophthalmol Vis Sci 2013;54:585-591.
35. Sujirakul T, Lin MK, Duong J, et al. Multimodal Imaging of Central Retinal Disease Progression in a 2-Year Mean Follow-up of Retinitis Pigmentosa. Am J Ophthalmol 2015;160:786-798.e4.
36. Robson AG, Tufail A, Fitzke F, et al. Serial imaging and structure-function correlates of high-density rings of fundus autofluorescence in retinitis pigmentosa. Retina 2011;31:1670-1679.
37. Robson AG, Michaelides M, Luong VA, et al. Functional correlates of fundus autofluorescence abnormalities in patients with RPGR or RIMS1 mutations causing cone or cone rod dystrophy. Br J Ophthalmol 2008;92:95-102.

38. Escher P, Tran HV, Vaclavik V, et al. Double concentric autofluorescence ring in NR2E3-p.G56R-linked autosomal dominant retinitis pigmentosa. Invest Ophthalmol Vis Sci 2012;53:4754-4764.
39. Comander J, Weigel-DiFranco C, Sandberg MA, Berson EL. Visual Function in Carriers of X-Linked Retinitis Pigmentosa. Ophthalmology 2015;122:1899-1906.
40. Verhoeven VJ, Wong KT, Buitendijk GH, et al. Visual consequences of refractive errors in the general population. Ophthalmology 2015;122:101-109.
41. Tideman JW, Snabel MC, Tedja MS, et al. Association of Axial Length With Risk of Uncorrectable Visual Impairment for Europeans With Myopia. JAMA Ophthalmol 2016;134:1355-1363.
42. Beltran WA, Cideciyan AV, Lewin AS, et al. Gene therapy rescues photoreceptor blindness in dogs and paves the way for treating human X-linked retinitis pigmentosa. Proc Natl Acad Sci U S A 2012;109:2132-2137.
43. Beltran WA, Hammond P, Acland GM, Aguirre GD. A frameshift mutation in RPGR exon ORF15 causes photoreceptor degeneration and inner retina remodeling in a model of X-linked retinitis pigmentosa. Invest Ophthalmol Vis Sci 2006;47:1669-1681.
44. Maguire AM, Simonelli F, Pierce EA, et al. Safety and Efficacy of Gene Transfer for Leber's Congenital Amaurosis. N Engl J Med 2008;358:2240-2248.
45. Jacobson SG, Cideciyan AV, Ratnakaram R, et al. Gene Therapy for Leber Congenital Amaurosis caused by RPE65 mutations: Safety and Efficacy in Fifteen Children and Adults Followed up to Three Years. Arch Ophthalmol 2012;130:9-24.
46. Bainbridge J, Mehat M, Sundaram V, et al. Long-Term Effect of Gene Therapy on Leber's Congenital Amaurosis. N Engl J Med 2015;372:1887-1897.
47. Edwards TL, Jolly JK, Groppe M, et al. Visual Acuity after Retinal Gene Therapy for Choroideremia. N Engl J Med 2016;374:1996-1998.

SUPPLEMENTAL MATERIAL

Supplemental Digital Content 1. Data collected for patients with *RPGR*-associated retinal dystrophies

Retrieved data	RP patients, n (%)	COD/CORD patients, n (%)
Longitudinal data available	46 (88)	21 (95)
Only cross-sectional data available	6 (12)	1 (5)
Follow-up time ≥2 years	39 (75%)	18 (82)
Age at onset first symptom	25 (48)	20 (91)
Visual acuity	49 (94)	21 (95)
Refractive error	45 (87)	20 (91)
Electroretinogram pattern	30 (58)	18 (82)
Goldmann visual field	25 (48)	6 (27)
Fundus autofluorescence	15 (29)	11 (50)
OCT	15 (29)	12 (55)
Heidelberg SD-OCT	14 (27)	11 (45)
Zeiss	-	1 (5)
Topcon	4 (8)	-

RP, retinitis pigmentosa; COD, cone dystrophy; CORD, cone-rod dystrophy; OCT, Optical Coherence Tomography; SD-OCT, Spectral Domain Optical Coherence Tomography.

Supplemental Digital Content 2. Mutations in the *RPGR* gene found in this cohort

Diagnosis	Exon	Nucleotide	Protein	N patients (n families)	Reference
RP	1	c.27del	p.(Asp10Ilefs*58)	7 (1)	This study
RP	3	c.248-28_248-10del	p.(?)	1 (1)	This study
RP	5	c.423del	p.(Ile142Leufs*14)	1 (1)	This study
RP	5	c.425T>G	p.(Ile142Ser)	3 (1)	This study
RP	6	c.485_486del	p.(Phe162Tyrfs*4)	1 (1)	Sharon et al. 2000
RP	7	c.706C>T	p.(Gln236*)	1 (1)	Buraczynska et al. 1997
CORD/RP*	10	c.1246-?_*1091-?	Deletion after exon 10	3 (2)	This study
RP	11	c.1345C>T	p.(Arg449*)	2 (1)	Breuer et al. 2002; Demirci et al. 2003
RP	14	c.1573-?_1753+?del	p.(Lys525Argfs*17)	1 (1)	This study
RP	ORF15	c.1773_1776del	p.(Gly592Glnfs*9)	1 (1)	This study
RP	ORF15	c.2236_2237del	p.(Glu746Argfs*23)	5 (4)	Vervoort et al. 2000
RP	ORF15	c.2237_2241del	p.(Glu746Glyfs*22)	2 (1)	This study
RP	ORF15	c.2323_2324del	p.(Arg775Glufs*59)	2 (1)	Breuer et al. 2002
RP	ORF15	c.2362_2366del	p.(Glu788Argfs*45)	4 (2)	This study
RP	ORF15	c.2405_2406del	p.(Glu802Glyfs*32)	9 (4)	Vervoort et al. 2000; Breuer et a.l 2002; Andreasson et al. 2003
CORD	ORF15	c.2426_2427del	p.(Glu809Glyfs*25)	3 (1)	Vervoort et al. 2000, Breuer et al. 2002; Andreasson et al. 2003; Jin et al. 2006
RP	ORF15	c.2730_2731del	p.(Glu911Glyfs*167)	1 (1)	Vervoort et al. 2000
RP	ORF15	c.2838_2839del	p.(Glu947Glyfs*131)	1 (1)	Pelletier et al. 2007
RP	ORF15	c.2840dup	p.(Glu949Glyfs*130)	4 (1)	Neidhardt et al. 2008
COD	ORF15	c.2950G>T	p.(Glu984*)	1 (1)	This study
CORD/RP*	ORF15	c.2959G>T	p.(Glu987*)	3 (1)	This study
RP	ORF15	c.2964_2965del	p.(Glu989Glyfs*89)	1 (1)	Garica-Hoyos et al. 2006
RP	ORF15	c.2993_2996del	p.(Glu998Glyfs*90)	3 (1)	Vervoort et al. 2000
RP	ORF15	c.3011_3012del	p.(Glu1004Glyfs*74)	1 (1)	Sharon et al. 2003
COD	ORF15	c.3039_3040del	p.(Glu1014Glyfs*64)	1 (1)	Zahid et al. 2013

*Multiple diagnoses within one family.

Nucleotide changes in cDNA are noted with transcript NM_001034853.1 as reference.

COD, cone dystrophy; CORD = cone-rod dystrophy; RP, retinitis pigmentosa.

Supplemental Digital Content 3. Patients with asymmetry in visual acuity

Study ID	Diagnosis	Presumed cause of asymmetry
11	RP	Unknown
15	RP	Recurring anterior uveitis in the worse seeing eye after an exudative retinal detachment due to extensive neovascularization
20	RP	Unknown
28	RP	Unknown
51	RP	Amblyopia, potentially due to strabismus or anisometropia (SER OD -8.625D; OS -7.125D)
62	RP	Unknown
66	RP	More atrophy of the EZ and ELM in the worse seeing eye
72	RP	ERM and subtly more EZ atrophy in the worse seeing eye
76	RP	Unexplained episodes of transient stabbing pain in the worse seeing eye with variable effect on BCVA
95	RP	Unknown
104	RP	Anisometropia, which may point to amblyopia (SER OD -13.5; OS -12.0D)
89	CORD	Unknown, but the worse seeing eye has more extensive peripapillary atrophy
120	CORD	Unknown, subtly more EZ atrophy in the worse seeing eye
131	CORD	Anisometropia, which may point to amblyopia (SER OD -7.25; OS -4.75D)
190	COD	More ELM attenuation in the worse seeing eye

BCVA, best corrected visual acuity; ELM, external limiting membrane; ERM, epiretinal membrane; EZ, ellipsoid zone; ONL, outer nuclear layer; SER, spherical equivalent of the refractive error.

In 3 RP patients (6%), one eye was consistently the better seeing eye by 2-3 Snellen lines until the ages of 14, 18, and 32 respectively, followed by a 10-year period of symmetry in the 14-year old patient, after which the other eye became the better seeing eye by 1-3 lines in all 3 patients. In 1 CORD patient, the left eye was consistently the better seeing eye by 1-3 lines until the age of 76, after which a period of symmetry ensued, followed by the right eye becoming the better seeing eye by 1-3 lines.

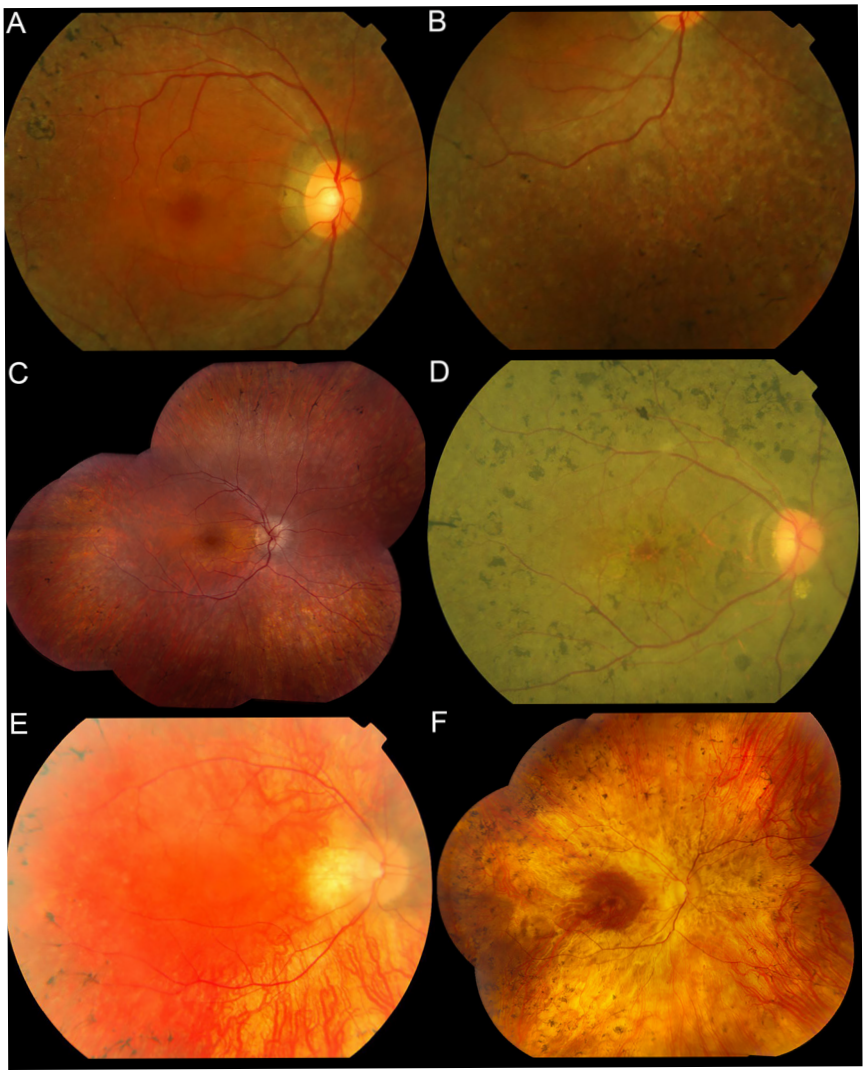

Supplemental Digital Content 4. Fundus photographs of patients with *RPGR*-associated retinitis pigmentosa. **A-B.** Fundus of a 30-year-old Asian patient with a pathogenic frameshift mutation (c.2405_2406del; p.(Glu802Glyfs*156)) in *RPGR*-ORF15 (BCVA in the right eye 20/100; in the left eye 20/67), showing peripapillary atrophy, retinal pigment epithelium atrophy, bone spicule pigmentation in the midperiphery, and yellow-white lesions resembling pseudoreticular-like drusen (arrowhead). **C.** Fundus of a 19-year-old Caucasian patient with a missense mutation (c.425T>G; p.(Ile142Ser)) in exon 5 of *RPGR* (BCVA in the right eye 20/25; in the left eye 20/20), showing a pale optic disc with pseudopapilledema due to optic disc drusen, relative sparing of the foveal retinal pigment epithelium, and scattered bone spicule pigmentation in the (mid-)periphery. **D.** Fundus of a 44-year-old patient with a pathogenic frameshift mutation (c.2405_2406del; p.(Glu802Glyfs*156)) in *RPGR*-ORF15 (BCVA in the right eye 20/100; in the left eye 20/1200) showing atrophic retinal pigment epithelium alterations and coarse hyperpigmentation outside and inside the posterior pole, with an astrocytic hamartoma near the optic disc, which was only found in his right eye. **E.** Fundus of a 28-year-old patient with a frameshift mutation (c.2359_2363del;

p.(Glu788Argfs*45)) in *RPGR*-ORF15 (BCVA in the right eye 20/50; in the left eye 20/67), showing a pale optic disc with temporal peripapillary atrophy, relatively intact retinal pigment epithelium in the posterior pole, and bone spicule pigmentation outside of the vascular arch. **F.** Fundus of a 42-year-old patient with a pathogenic frameshift mutation (c.27del; p.(Asp10Ilefs*58)) in exon 1 (BCVA in both eyes 20/63), showing a pale optic disc, relatively spared retinal pigment epithelium in the fovea surrounded by a ring of atrophy, coarse and bone spicule pigmentations, and visible choroidal vessels in the periphery due to extensive retinal pigment epithelium atrophy.

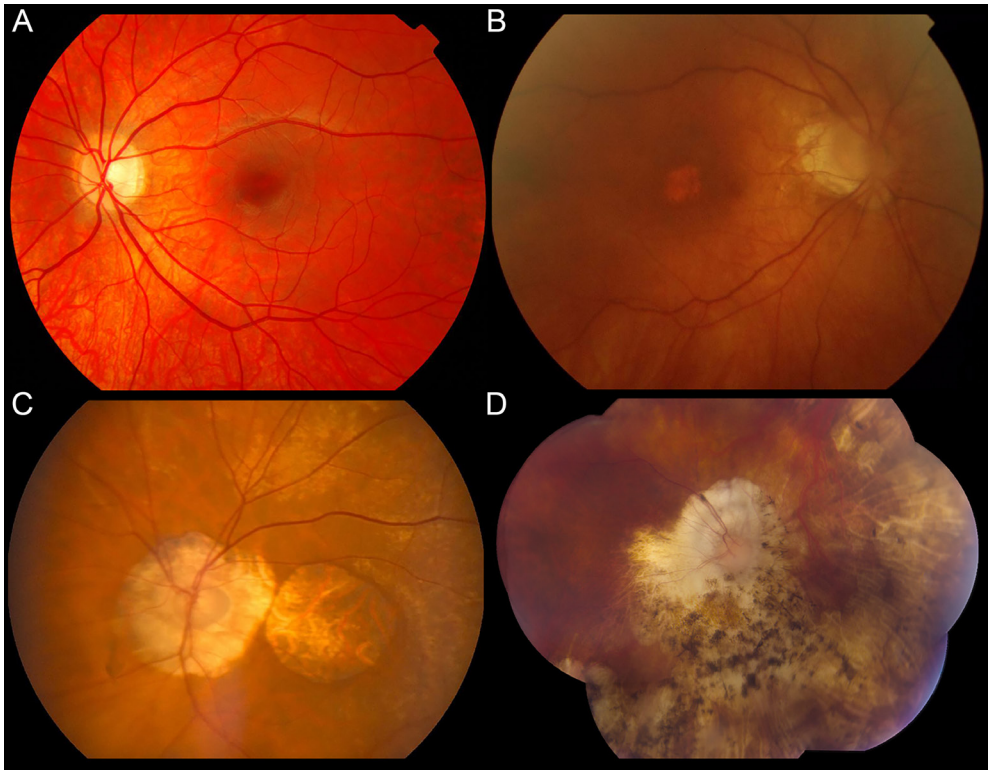

Supplemental Digital Content 5. Fundus photographs of patients with *RPGR*-associated predominantly cone-involving dystrophies. A. Fundus of a 19-year-old COD patient (BCVA in both eyes 20/50) carrying a c.3317dup (p.(Ser1107Valfs*4)) mutation in *RPGR*-ORF15, showing mild mottling alterations of the retinal pigment epithelium in macula, and mild optic disc pallor. **B.** Fundus of a 75-year-old CORD patient with a frameshift variant (c.3300_3301del; p.(His1100Glnfs*10)) in *RPGR*-ORF15 (BCVA in both eyes 20/125), showing peripapillary atrophy and a small region of atrophy in the central macula, surrounded by mild retinal pigment epithelium alterations. The periphery, not depicted here, showed fine salt-and-pepper pigmentation. **C.** Colour fundus photograph of a 79-year-old COD patient (BCVA in the right eye 20/400; in the left eye 2/100) carrying a c.3317dup (p.(Ser1107Valfs*4)) mutation in *RPGR*-ORF15, with sharply demarcated profound chorioretinal and retinal pigment epithelium atrophy in the macula and around the optic disc. In the posterior pole and around the retinal vessels, small and densely packed drusenoid deposits were also visible. **D.** Fundus of an 88-year-old CORD patient with a frameshift mutation (c.3092del; p.(Glu1031Glyfs*58)) in *RPGR*-ORF15 (BCVA in the right eye 20/320; in the left eye 2/100), showing profound atrophy of the retinal pigment epithelium and coarse hyperpigmentation nasally and inferiorly reaching into the macula and around the optic disc.

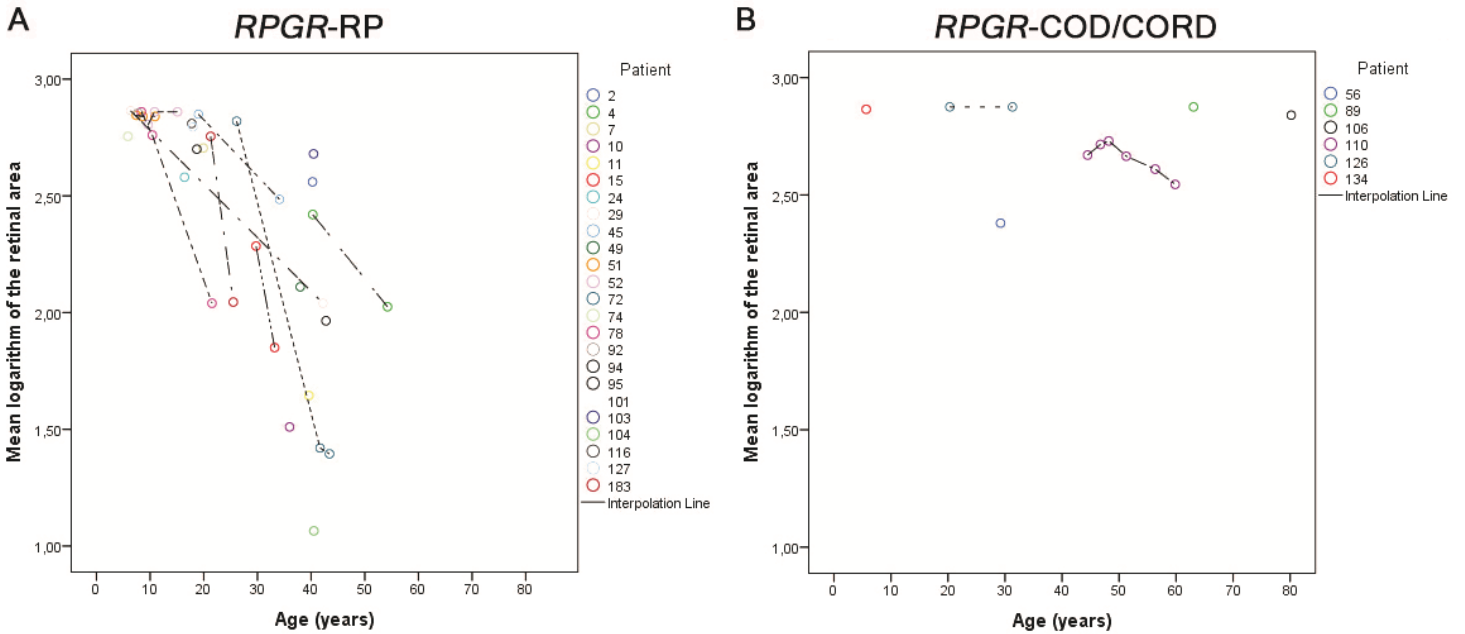

Supplemental Digital Content 6. Individual visual field areas of patients with *RPGR*-associated retinitis pigmentosa (A) and predominantly cone-involving dystrophies (B).